The Effect of Nickel Coating on Stainless steel 316 on Growth of Carbon Nanotube from Polypropylene Waste

Praswasti P.D.K.Wulan
Department of Chemical Engineering, Faculty of Engineering, Universitas Indonesia

Juli Ayu Ningtyas
Sustainable Energy Research Group, Department of Chemical Engineering, Faculty of Engineering, Universitas Indonesia

Hasanah, Miranda
Sustainable Energy Research Group, Department of Chemical Engineering, Faculty of Engineering, Universitas Indonesia

https://doi.org/10.5109/2328411

出版情報：Evergreen. 6 (1), pp.98-102, 2019-03. Green Asia Education Center
バージョン：
権利関係：

The Effect of Nickel Coating on Stainless steel 316 on Growth of Carbon Nanotube from Polypropylene Waste

Praswasti P.D.K.Wulan[1,*], Juli Ayu Ningtyas [2], Miranda Hasanah[2]

[1] Department of Chemical Engineering, Faculty of Engineering, Universitas Indonesia, Kampus UI-Depok, Jawa Barat 16424, Indonesia

[2] Sustainable Energy Research Group, Department of Chemical Engineering, Faculty of Engineering, Universitas Indonesia, Kampus UI-Depok, Jawa Barat 16424, Indonesia

Email: wulan@che.ui.ac.id

(Received January 30, 2019; accepted March 26, 2019)

This paper aims to obtain the effect of nickel coating on the wet impregnation method on 316 stainless steel (SS 316) catalytic substrate which received initial treatment with Oxidative Heat Treatment (OHT) using a flame synthesis reactor with a carbon source of polypropylene (PP) waste on the growth of carbon nanotubes (CNT). Nickel coating on SS 316 is intended to improve the quality and quantity of CNT that have not been obtained in previous studies. Variations in nickel loading are 5% and 10%. The results showed nickel coating could increase CNT yield by only 8.4%. However, the CNT produced from nickel coating on SS 316 substrates have better quality. The characterization of XRD showed that the peak intensity of the CNT is at $2\theta = 26^{o}$ and 43^{o}. This CNT still contained some impurities in the form of amorphous carbon such as Fe_3O_4 and Fe_3C. The effect of heating at high temperatures on the nickel layer resulted in the presence of NiO compounds in CNT samples. SEM results showed that there were still amorphous carbon and other impurities as detected in the XRD results. The characterization of EDX supported the XRD results which show that there was no significant percent mass increase in carbon. In TGA results, the nickel layer could increase the thermal stability of the CNT because the CNT has a percentage decrease in mass at 620^{o}C oxidation temperature. The best CNT results shown in nickel coating are 10% both regarding yield and quality because the substrate surface can prepare contact space between the active core and the reactants so that more CNTs will grow on the surface.

Keywords: CNT, Nickel, Polypropylene, SS 316, Wet Impregnation

1. Introduction

Plastic waste is a serious environmental problem because there is an increase of 500,000 tons/year. Nineteen percent (19%) of the type of plastic waste is a type of polypropylene. Polypropylene (PP) plastic waste began to expand in the field of nanotechnology because the carbon contained is more than the plastic type HDPE, LDPE, and PET, which is 86.7% [1]. These high carbon sources can be used to produce carbon nanotubes (CNT) [2].

CNT like diamond are probably the most well-known carbon allotrope. Hard amorphous carbon, called carbon like the diamond, has attracted attention as an alternative coating material to diamond [3]. CNT are 1/50,000th the width of a human hair, considerably smaller than a (commercial) diamond or perhaps even diamond dust grains. Therefore, it can be applied in the electronics industry, material industry, and hydrogen storage technology. However, there is still a lack of CNT production in Indonesia due to high production costs. The use of economical raw materials such as polypropylene as a carbon source for CNT synthesis will affect increasing economic potential.

Since 2013, the Universitas Indonesia's Department of Chemical Engineering had begun conducting researches on CNT made from plastic waste using the pyrolysis-synthesis method. The results of this study did not obtain CNT. Therefore, a flame synthesis reactor was developed with a stainless-steel catalyst preparation using the Oxidative Heat Treatment (OHT) method. The OHT method is a catalyst pretreatment in the form of heating in oxidative conditions, to produce CNT with a high yield that is capable of uncovering a layer of metal alloy on stainless steel (especially Fe) which is still covered by a layer of chrome. Usage of the stainless steel 316 because of its low price and high corrosion resistance [4]. Wulan et al. (2018) conducted a study on the effect of temperature and polypropylene pyrolysis time on the growth of CNT. The Optimal pyrolysis temperature was obtained at 525^{o}C for 45 minutes with a yield of 5.4 grams. However, the yield

and quality of CNT produced on the substrate were still not optimum, because the CNT was more oriented to the reactor wall. This orientation occurs because the reactor wall absorbs higher heat energy. Also, the CNT produced contains impurities such as Fe_2O_3, Fe_3O_4, Fe_3C, and amorphous carbon, due to the interaction between oxygen and Fe metal [5]. Coating nickel catalysts may solve these problems on SS 316 wired mesh substrates obtained from OHT [6]. Nickel catalysts can increase the reactivity of C-C and C-H bonds, making them useful for polymer cracking Ni catalysts are more stable and homogeneous than Fe, and produce good CNT quality with a high purity level and smaller crystal diameter [7]. The method chosen for coating stainless steel substrates with nickel is the wet impregnation method. The wet impregnation method was selected because of its simple technique and produces many active phase precursors because metal salts are more accessible to migrate from the solution into the pore. By using the wet impregnation method, we can also tailor the metal. Therefore, in this research, the nickel coating on SS 316 substrates resulted from Oxidative Heat Treatment with various loading was done to obtain CNT from polypropylene plastic waste.

2. Materials and Method

Pre-treatment of Stainless-Steel Catalytic Substrate

Ten grams of polypropylene were washed and then cut into 2 x 2 cm. Stainless steel (SS) 316 wired mesh was cut into squares with a size of 16x18 cm and then mechanically rubbed using isopropanol. SS 316 was then rolled with a diameter of 5 cm and placed into the furnace at 800°C for Oxidative Heat Treatment. After that, the stainless steel was immersed into an impregnation solution containing nickel nitrate hydrate $Ni(NO)_3.6H_2O$ with distilled water maintained at Ph = 3, then heated at 90°C for 8 hours and dried at 105°C for 4 hours. The final step of the preparation is the calcination process by heating at 900°C [8]. Variations in the loading of nickel are carried out at 0%, 5%, and 10% and was labeled as SS0, SS5, and SS10 of substrate sample.

Synthesis of Carbon Nanotube

Polypropylene plastics were placed into a boat inside of the pyrolysis reactor. Stainless steel substrate rolls were placed in the Argon synthesis reactor flowed to the reactor with 100 ml/min, while oxygen flowed at a rate of 33.3 ml/minute. The temperature of pyrolysis was set at 450 °C, while the temperature of the synthesis was set at 800 ° C for an hour. The temperature is set at the temperature control in each reactor. Temperature at the surface of the catalyst particle and the structure and type of catalyst particle are the key controlling parameters for growth of nanotubes in the flame synthesis process [9]. Flame synthesis is an auto-thermal process that is capable of providing temperature optimal for achieving desired synthesis condition [9].

Substrate and CNT Characterization

Catalyst samples from pre-treatment process were characterized using SEM and EDX (Energy Dispersive X-ray) Spectroscopy. The purpose of catalyst characterization using SEM is to determine the morphology of the surface of SS catalyst attached to nickel. The goal of EDX characterization is to determine the amount of metal that can stick to the surface of Stainless steel catalysts. Characterization test was carried out in the form of Powder X-ray diffraction (XRD) patterns a Phillips analytical X-Ray model number BV-2500 analysis. XRD to identify the existence and structure of CNT. A Hitachi and JEOL JSM 6510 LA Scanning Electron Microscopy (SEM) equipment (Japan) to determine the structure of CNT. The Energy Dispersive X-ray Spectroscopy (EDX) to determine the composition and weight percentage contained in CNT. TGA (Thermo Gravimetric Analysis) Perkin Elmer STA 6000 to identify the purity of the CNT and their thermal stability [10].

3. Results and Discussions

Characteristic of Substrate Catalyst

Figure 1 below shows the results of SEM from a 316 wired mesh stainless steel substrate with various treatments. From the three images, there are differences in morphology and surface area. Figure 1 (a) showed SS 316 without nickel coating. In Figure 1 (b) and (c) it can be seen that SS 316 underwent an attachment process, or stainless steel was coated with a nickel catalyst. The distribution of nickel attachment looks more evenly distributed in the SS5 sample, while the 10% nickel loading shows the accumulation of particles in certain areas along with some grooves. The grooves mean there is a greater surface area that affects the distribution of active nuclei [11]. This large surface area prepares the contact space between the active core and the reactants so that more CNTs will grow on the surface [12].

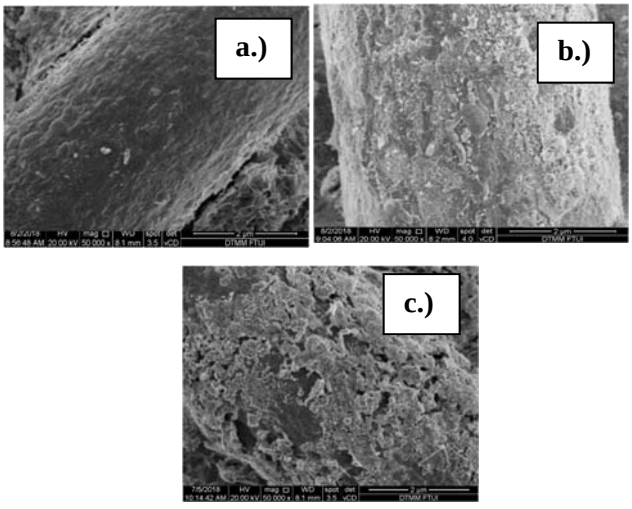

Fig 1 Surface morphology of a.) SS0 b.) SS5 and c.) SS10

EDX Surface Catalytic results can be used to determine the composition and weight percentage of elements contained in the stainless-steel substrate [13].

Table 1 showed EDX results, a SS-substrate that has been pre-treated with OHT without nickel coating (SS0) has a nickel composition of 3.86%. For substrate SS5 and SS10, the composition of nickel was 8.52% and 13.94% respectively. Due to an increase in Ni concentration, nickels were incorporated at the substrates. Fe concentration in each sample decreased with increasing number of nickel loading. Fe and Ni will be the catalysts for CNT growth with two active cores of Fe and Ni [14]. The presence of carbon compounds in each sample due to stainless steel is one type of steel that is a mixture of Fe and C so that element C will remain with almost the same percentage.

Table 1 Compositions and %-weight of the catalytic substrate

Element	Compositions (%-weight)		
	SS0	SS5	SS10
Ni	3.86	8.52	13.94
Fe	42.67	39.71	36.54
C	4.27	4.76	4.65
Cr	15.33	15.11	13.2
O	32.41	31.90	31.67

The presence of C on the substrate can also cause the existence of Fe_3C compounds which results in impurities in the CNT product [15]. The presence of Cr atoms on each SS-substrate indicates that the OHT and impregnation processes cannot significantly remove the chrome. The O concentration in all three samples was still relatively high. Atom O can form oxygen that found on the substrate after preparation because the oxidative heat treatment method is carried out in the presence of air [16]. Oxygen plays a role in breaking down the surface of the substrate to form a more reactive surface for CNT formation [17].

CNT Yield Analysis

Table 2 below shows the yields of each CNT sample.

Table 2. Yield of CNT

Sample	Mass of CNT on the substrate (gram)	Mass of CNT on the reactor wall (gram)	The total mass of CNT (gram)	Yield (%)
CNT SS0	1.30	1.22	2.52	36.0
CNT SS5	1.68	1.29	2.89	41.2
CNT SS10	1.94	1.17	3.11	44.4

From the CNT yield data above, the highest yield value is found on CNT with a substrate coated with 10% nickel loading, which is 44.4%. However, this value does not show a significant yield difference compared to CNT with a substrate covered with 5% nickel loading. The difference in yield from the two samples is only 3.2%. Meanwhile, the total increase in the yield of free nickel coating samples subject to a 10% nickel coating experienced an increase in yield of around 8.4%. The yield produced is considered not comparable to the resources and production costs that are high enough for nickel coating. According to Yao's research (2017), increasing the composition of Ni as a catalyst does not result in a significant increase in carbon deposits. Fe catalysts produce increased carbon deposits. Lim (2017) stated that higher CNT yields could be used apart from impregnation, such as using synthesis and hydrocarbon sources.

Characteristics of CNT

Figure 2 below shows the results of CNT characterization using XRD on each raw material and each sample variation.

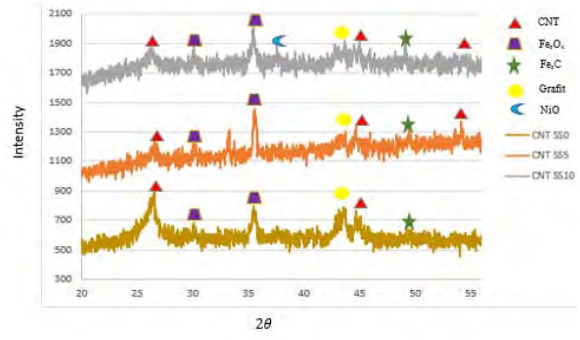

Fig 2. XRD Pattern of CNT samples

XRD characterization indicates that CNT was formed in every variation of nickel loading on each substrate. The peak intensity means this at an angle of 2θ for CNT, which is 26° and 43° [18]. The peak intensity of CNT is obtained on the substrate with 10% nickel loading. In addition to the peak CNT, there are several peaks which indicate the presence of impurities on the CNT produced in each variation such as Fe_3O_4, Fe_3C, and graphite. The peak intensity at an angle of 2θ for Fe3C compounds was 38 ° and 41 °[19]. For Fe_3O_4 compounds which are 30 ° and 35, graphite is shown at an intensity peak of 43.7 ° [20]; and for amorphous carbon, it is 45 °, 58.5 °, and 77 °. Graphite detection at XRD peak indicates an incomplete formation of MWCNT. Also, the presence of peaks at 2θ = 37.8° indicated the presence of NiO compounds for CNT SS10 samples. NiO compounds were also formed in PPT based CNT samples with 10% nickel-coated substrate. The formation of NiO compounds was due to the high-temperature heating process in the presence of oxygen, reacting to form NiO compounds. In this study, high-temperature heating occurs in two processes, which were

calcination and CNT synthesis process in the reactor, allowing the NiO compound to form on the substrate after the impregnation process or before the CNT synthesis process in the reactor [21].

From the results of the diffractogram shown in Figure 2, the crystal size of the CNT can be determined by the Scherrer Equation below.

$$D = \frac{K\lambda}{B\cos\theta}$$

With D being the average crystal size of CNT (nm), K is the Scherrer constant, λ is the X-ray (nm) wavelength, B is the FWHM value (Full Width at Half Maximum), and θ is the Bragg angle. The K value shows the sphericity of the analyzer crystals. Generally, the K value used in the analysis of CNT samples is 0.9. The amount of B is obtained from the difference in Bragg angle at a peak intensity of half the maximum peak intensity [22].

Table 3. Crystal diameter of CNT

Sample	Crystal diameter of CNT (nm)
CNT SS 0	12.64
CNT SS5	6.95
CNT SS10	6.48

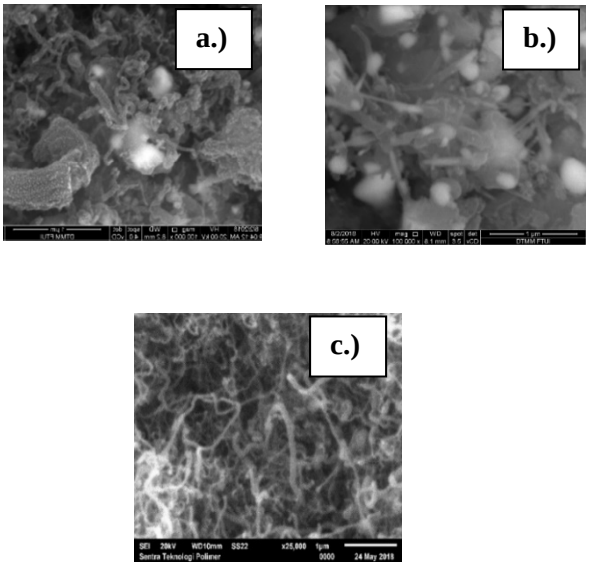

Fig 3 CNT morphologies by SEM Characterisation of a.) CNT SS0, b.) CNT SS5, c.) CNT SS10

Table 3 shows the calculation results of the diameter of the CNT. The lowest crystal diameter value is produced by CNT based on PP waste with 10% nickel loading. The largest diameter of crystals produced by CNT is based on PP waste with substrate without nickel coating. Large crystal diameters are caused by the formation of carbon aggregates which can increase the size of the CNT. Nickel coating affects the average crystal diameter of CNTs.

Figure 3 showed the results of SEM characterization for CNT on various substrate variations. The results showed the number of impurities contained in CNTs which are characterized by light aggregates and non-tubular carbon forms. Through SEM characterization, CNTs can be seen which are characterized by tubular parts in all variations. CNTs that grow on all varieties have entangled CNT bundles. The CNT produced in this study has a tips growth method characterized by the presence of catalysts at the ends of tubular tubes [23].

Also, impurities that are dominated by amorphous carbon are also seen in all variations that are characterized by light aggregates. As shown in the XRD results, other impurities seen in SEM in the form of iron oxide in the structure of Fe_2O_3 derived from SS 316 fall out which are marked by flakes and also excessive Fe content in carbon sources [24]

Fe particles will dominate CNT growth. In sample SS5, there was also a formation of a long tubular nanotube, but Fe particles were also encapsulated in the CNT which caused lumps of impurities detected in XRD. In each variation, SEM images show the presence of integrated CNTs with many impurities such as amorphous carbon, graphite, and low-quality carbon. This happens because carbon sources have not entirely decomposed. The formation of agglomerated nanocarbon materials is also caused by high catalyst concentration and uneven distribution of catalysts in the synthesis reactor.

Table 4 The compositions of CNT

Component	CNT SS0	CNT SS5	CNT SS10
C (%-wt.)	55.71	73.70	74.07
O (%-wt.)	4.02	5.17	5.63
Fe (%-wt.)	30.10	12.48	1.54
Ni (%-wt.)	10.17	8.42	17.26

Table 4 showed the most carbon compounds produced was on the substrate with 10% nickel coating because nickel can create more carbon deposit. Also, there are several other types of elements that are detected through EDX from samples of variations in the nature and placement of substrates, namely O and Fe atoms. Atom O is the output of the preparation using the OHT method and is caused by oxidation of the reactor walls at high temperatures in the form of Fe_2O_3 and Fe_3O_4 CNT SS10 samples show much less content of Fe atoms than other samples. This indicates that the nickel coating affects the concentration of Fe when CNT is formed. Nickel as a catalyst will dominate the work of the CNT growth catalyst so that a higher carbon deposit is produced along with the nickel catalyst addition. [25]

The level of CNT purity is directly proportional to the temperature of CNT oxidation. The temperature of the CNT oxidation can be detected by decreasing the percentage of the mass of the sample at a certain

temperature when analyzed with a TGA instrument. Based on the results obtained, Figure 4 can be seen that the highest CNT purity is produced from CNT that grows on the substrate with 10% nickel loading. The percentage reduction in mass at a temperature of 250-450ºC formed amorphous nanocarbon, while at higher temperatures of 500-600ºC, the types of nanocarbon built was filaments.

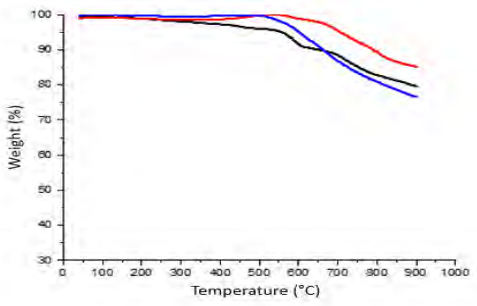

Fig 4. TGA pattern of CNTs

The percentage of mass is oxidized at a temperature of 600-750ºC typically build MWCNT type of nanocarbon [26]. In PP-based CNT that grow on the substrate without the nickel coating, the percentage decrease in sample mass begins to occur at an oxidation temperature of around 375ºC. For CNT SS5 and SS10, there was a significant percentage reduction in mass at temperatures of approximately 515ºC and 620ºC. This proves that the types of nano-carbons that are formed in most CNT SS0 that are detected are amorphous carbon types, and filaments are detected on CNT SS5. CNT in SS10 mostly forms MWCNT.

4. Conclusions

Nickel Coating on SS-316 catalytic substrates in this study has not been too significant to increase the yield of the CNT produced. The quality of CNT with PP carbon waste sources has increased with the presence of a nickel coating on SS catalyst substrates. The crystalline diameter of the formed CNT was smaller than the previous study which was 6.48 nm. The higher thermal stability became oxidized at 620ºC. The highest yield and the most effective quality of CNT were obtained at the 10% nickel loading catalyst. This loading can produce a large surface area to prepare contact spaces between active site catalyst and reactants. Further research needs to be done on Fe coating as the main content on SS 316 to increase the yield of CNT with PP waste carbon sources becomes oxidized at 620ºC. The highest yield and because it can produce a large surface area to prepare contact spaces between active site catalyst and reactants.

Acknowledgments

The authors would like to thank for the research funding from The Directorate General of Higher Education, the Indonesian Ministry of National Education under Penelitian Dasar Unggulan Perguruan Tinggi with Contract Number: 416/UN2.R3.1/ HKP05.00 /2018.

References

1) E. S Parparita., *J Mater. Cycles Watse.*, **4**, 101-114 (2014).
2) C. Zhuo, B. Hall, R. Henning, Y. Levendis, *Carbon*, 48, 4024-4034 (2010)
3) Hiroshi Naragino, Mohamed Egiza, Aki Tominaga, Koki Murasawa, Hidenobu Gonda, Masatoshi Sakurai, Tsuyoshi Yoshitake, *EVERGREEN Joint Journal of*, 3 (1), 1-5, March (2016).
4) P.P.D.K Wulan and S.B Wijardono, *Int. J. Adv. Sci. Eng. Inf. Technol.*, **7 (2)**, 552-558. (2017).
5) P.P.D.K Wulan., J.D. Sidauruk., J.A. Ningtyas, *E3S Web of Conference*, **67**, 03030 (2018).
6) R.T.K. Baker, M.A. Barber, P.S. Harris, F.S. Feates, R.J. Waite, *J. Catalysis*, 26, 51 – 62 (1972)
7) D. Yao, C. Wu, H. Yang, Y. Zhang, M.A. Nahil, Chen, Y., P.T. William., H. Chen. *J. Energy Convers*., (2017)
8) I. Anzel, *J. Metal*, 4, 325-336 (2007)
9) J.P. Gore, A. Sane, Tesis, Indiana: Purdue University (2011)
10) O.C. Carneiro, N.M. Rodriguez, R.T.K. Baker, *Carbon*, 43, 2389-2396 (2005)
11) M. Kumar, *Carbon*, 5, 147-170 (2011)
12) J.C. Acomb., C. Wu, P.T. Williams. *Appl. Catalysis B: Env*, 147, 571-584 (2013)
13) J. Liu, Z. Jiang, H.Yu, T. Tang, *Polymer Degradation and Stability*, 96, 1711 – 1719 (2011)
14) U. Weissker, S. Hampel, A. Leonhardt, B. Buncher, *J. Mat.*, 3, 4387 – 4427 (2010)
15) M. Zhang, J. Li, *Materials Today*, 12, 12-18 (2015)
16) Y.K. Yap, V. Kayastha, S. Hackney, S. Dimovski, Y. Gogotsi, *Materials Research Society Symposium Proceedings*, 818, 1-6 (2004)
17) R. X. Yang, K.H. Chuang, M.Y. Wey, *J. Energ Fuels*, 1, 1-53 (2015)
18) S. Mopoung. *Intl J. Phys. Sci*., **6 (**7), 1789 – 1792 (2011)
19) A.G. Osorio and Bregman. *J. Appl. Sci*., **5**, 123-130. (2013)
20) M.R. Hosseini, & J. Nader. *ASME International Mechanical Engineering Congress and Exposition*. (2007)
21) J. Sengupta, C. Jacob. *J. Nano. Res.*, 12, 457 – 465 (2010)
22) E. Skretzuka, M. Pulchaski, I. Krunciska, *Sensors*, 14, 16816 – 16828 (2014)
23) K.A. Shah, B. A. Tali, *Mat Sci Semicond Proc*, 4, 67-82 (2015)
24) Y.D. Lim, *J. Appl. Sci.*, **2**, 6063-6071 (2017).
25) C. Zhuo, *J Surf. Sci*., 1 – 6. (2014).
26) R.X. Yang, K.H.Chuang, M.Y. Wey. *J Energ. Fuels*, **1,** 1-53 (2015).